JCN Open Access ORIGINAL ARTICLE

pISSN 1738-6586 / eISSN 2005-5013 / J Clin Neurol 2022;18(4):437-446 / https://doi.org/10.3988/jcn.2022.18.4.437

[^{18}F]THK-5351 PET Patterns in Patients With Alzheimer's Disease and Negative Amyloid PET Findings

Minyoung Oh[a], Jungsu S. Oh[a]
Seung Jun Oh[a], Sang Ju Lee[a]
Jee Hoon Roh[b], Woo Ram Kim[c]
Ha-Eun Seo[c], Jae Myeong Kang[d]
Sang Won Seo[e], Jae-Hong Lee[b]
Duk L. Na[e], Young Noh[c,f]
Jae Seung Kim[a]

[a]Department of Nuclear Medicine, Asan Medical Center, University of Ulsan College of Medicine, Seoul, Korea
[b]Department of Neurology, Asan Medical Center, University of Ulsan College of Medicine, Seoul, Korea
[c]Neuroscience Research Institute, Gachon University, Incheon, Korea
[d]Department of Psychiatry, Gil Medical Center, Gachon University College of Medicine, Incheon, Korea
[e]Department of Neurology, Samsung Medical Center, Sungkyunkwan University, School of Medicine, Seoul, Korea
[f]Department of Neurology, Gil Medical Center, Gachon University College of Medicine, Incheon, Korea

Received July 21, 2021
Revised December 28, 2021
Accepted December 29, 2021

Correspondence
Young Noh, MD, PhD
Department of Neurology, Gil Medical Center, Gachon University College of Medicine, 21 Namdong-daero 774beon-gil, Namdong-gu, Incheon 21565, Korea
Tel +82-32-460-3346
Fax +82-32-460-3344
E-mail ynoh@gilhospital.com

Jae Seung Kim, MD, PhD
Department of Nuclear Medicine, Asan Medical Center, University of Ulsan College of Medicine, 88 Olympic-ro 43-gil, Songpa-gu, Seoul, 05505, Korea
Tel +82-2-3010-4594
Fax +82-2-3010-4590
E-mail jaeskim@amc.seoul.kr

Background and Purpose Alzheimer's disease (AD) does not always mean amyloid positivity. [^{18}F]THK-5351 has been shown to be able to detect reactive astrogliosis as well as tau accompanied by neurodegenerative changes. We evaluated the [^{18}F]THK-5351 retention patterns in positron-emission tomography (PET) and the clinical characteristics of patients clinically diagnosed with AD dementia who had negative amyloid PET findings.

Methods We performed 3.0-T magnetic resonance imaging, [^{18}F]THK-5351 PET, and amyloid PET in 164 patients with AD dementia. Amyloid PET was visually scored as positive or negative. [^{18}F]THK-5351 PET were visually classified as having an intratemporal or extratemporal spread pattern.

Results The 164 patients included 23 (14.0%) who were amyloid-negative (age 74.9±8.3 years, mean±standard deviation; 9 males, 14 females). Amyloid-negative patients were older, had a higher prevalence of diabetes mellitus, and had better visuospatial and memory functions. The frequency of the apolipoprotein E ε4 allele was higher and the hippocampal volume was smaller in amyloid-positive patients. [^{18}F]THK-5351 uptake patterns of the amyloid-negative patients were classified into intratemporal spread (n=10) and extratemporal spread (n=13). Neuropsychological test results did not differ significantly between these two groups. The standardized uptake value ratio of [^{18}F]THK-5351 was higher in the extratemporal spread group (2.01±0.26 vs. 1.61±0.15, p=0.001). After 1 year, Mini Mental State Examination (MMSE) scores decreased significantly in the extratemporal spread group (-3.5±3.2, p=0.006) but not in the intratemporal spread group (-0.5±2.8, p=0.916). The diagnosis remained as AD (n=5, 50%) or changed to other diagnoses (n=5, 50%) in the intratemporal group, whereas it remained as AD (n=8, 61.5%) or changed to frontotemporal dementia (n=4, 30.8%) and other diagnoses (n=1, 7.7%) in the extratemporal spread group.

Conclusions Approximately 70% of the patients with amyloid-negative AD showed abnormal [^{18}F]THK-5351 retention. MMSE scores deteriorated rapidly in the patients with an extratemporal spread pattern.

Keywords [^{18}F]THK-5351; Alzheimer's disease; amyloid; neuropsychological test; positron-emission tomography.

INTRODUCTION

Alzheimer's disease (AD) is the most common form of dementia, accounting for 60%–70% of dementia cases.[1] Around 47 million people have dementia worldwide, and this number is expected to increase to 131 million by 2050.[2]

AD is diagnosed when certain core clinical criteria be satisfied.[3] However, a dementia diagnosis based on clinical criteria alone is not especially helpful in determining its histopathological cause. For example, the clinical diagnosis of probable AD shows only modest sensitivity (71%–81%) and specificity (approximately 70%) relative to postmortem ex-

aminations,[4,5] which can potentially confound clinical trials in AD.[6,7]

Amyloid positron-emission tomography (PET) measures the amount of amyloid-β aggregates—one of the pathological hallmarks of AD—in the brains of living subjects.[8-11] In 2018, the National Institute of Age−Alzheimer's Association (NIA-AA) shifted the definition of AD to a biological construct.[11] A recent meta-analysis found that the mean prevalence of amyloid positivity was 88% (95% confidence interval=85%−90%) in cases of AD dementia, and that it varied with age and apolipoprotein E (ApoE) ε4 status.[12] A negative amyloid PET scan was observed in 12% of clinically diagnosed patients with AD dementia, and was most common in older ApoE-ε4-negative patients.[12] The latter finding was consistent with those of two recent phase-3 trials on humanized anti−amyloid-β monoclonal antibodies.[6,7] The "AD phenocopy" was most prevalent in older and ApoE-ε4-negative participants, and may be explained by diverse age-related pathologies (e.g., hippocampal sclerosis, argyrophilic grain disease, or tangle-predominant dementia)[13-15] that preferentially target the limbic system, resulting in a memory-predominant presentation that may be mistaken for AD.

Off-target binding limits the specificity of [18F]THK-5351, which was initially found to target tau aggregates in neurofibrillary tangles,[16] but it has subsequently been shown to bind to monoamine oxidase B and glial fibrillary acidic protein.[17,18] Therefore, [18F]THK-5351 might reflect neuroinflammation in the brain. We aimed to determine the clinical characteristics and uptake pattern of [18F]THK-5351 PET in patients with amyloid-negative AD.

METHODS

Participants

Patients with AD dementia who had been diagnosed with probable AD according to the guidelines of the National Institute of Neurological and Communicative Disorders and Stroke and the AD and Related Disorders Association, and who also met the criteria recommended by the NIA-AA were recruited from the memory disorder clinics at Asan Medical Center, Gachon University Gil Medical Center, and Samsung Medical Center between January 2016 and August 2017.[3,19] The exclusion criteria in brain magnetic resonance imaging (MRI) were structural lesions such as territorial infarctions, intracranial hemorrhage, traumatic brain injury, hydrocephalus, severe white-matter hyperintensity (WMH) defined as D3P3 on the modified Fazekas scale,[20] or WMH associated with radiation, multiple sclerosis, or vasculitis. Secondary causes of cognitive decline were ruled out through laboratory tests that assessed complete blood counts, vitamin B12 and folate levels, thyroid function, the metabolic profile, and syphilis serology.

All participants completed the Seoul Neuropsychological Screening Battery, which assesses attention, visuospatial function, language, memory, and frontal executive function, and includes the Mini Mental State Examination (MMSE).[21] ApoE genotyping was performed in all participants, who also underwent amyloid (either [18F]florbetaben or [18F]flutemetamol) and [18F]THK-5351 PET and brain MRI.

After the PET scan, each patient was re-evaluated for their most-probable diagnosis of dementia according to the diagnostic criteria for frontotemporal dementia (FTD), subcortical vascular dementia, and diffuse Lewy body dementia, and were followed up accordingly.[22-25]

This study was approved by the Institutional Review Board of Asan Medical center (2016-0023), Gil Medical Center (GDIRB2015-272), and Samsung Medical Center (2015-09-880). Written informed consent was obtained from all participants.

Acquisition of PET data

We performed static brain PET scans on all participants at 50−70 min after an intravenous injection of 185 MBq of [18F]THK-5351 for tau and 90−110 min after an intravenous injection of 300 MBq of [18F]florbetaben or 185 MBq of [18F]flutemetamol for amyloid. A Discovery 690, 710, or 690 Elite PET/CT scanner (GE Healthcare, Chicago, IL, USA) was used at Asan Medical Center, a Siemens Biograph 6 Truepoint (Siemens, Munich, Germany) was used at Gil Medical Center, and a Discovery STE PET/CT scanner (GE Healthcare, Chicago, IL, USA) was used at Samsung Medical Center. Three-dimensional Hoffman phantom PET image-based harmonization was conducted to identify the optimal size for the smoothing kernel to match the resolution of the digital gray matter (GM)/white matter (WM) segmentation with that of each PET scanner. Thereafter, we identified an optimal smoothing kernel that matched the spatial resolution of all scanners to that of the scanner with the lowest resolution; that is, the Discovery STE device (detailed methods are described at Joshi et al.[26]).

Visual analysis of PET data

To evaluate [18F]THK-5351 binding in the brain, a visual grading was performed by two board-certified nuclear medicine physicians (M.O and J.S.K.) blinded to the patients' clinical information. The goal of each read was to identify and locate areas in the brain exhibiting [18F]THK-5351 activity greater than that in the cerebellum. Retention patterns were visually classified into intratemporal spread (no retention or retention only within the temporal cortex [WT]) and extratemporal

spread (retention in the frontotemporoparietal cortex [FTP], retention in the frontotemporal cortex [FT], or diffuse retention in the frontotemporoparietal WM rather than in the GM [FTP-WM]) (Fig. 1). This is a modification of the classification applied to the distribution pattern of flortaucipir and [^{18}F]THK-5351 PET.[27,28]

The amyloid PET scans demonstrating either [^{18}F]florbetaben or [^{18}F]flutemetamol uptake in the brain were assessed visually using a binary classification (positive or negative) as recommended for each tracer.[29,30]

Quantitative analysis of PET data

Each participant's PET image was strictly coregistered to their magnetization-prepared rapid gradient-echo data using the SPM12 tool (Wellcome Trust Centre for Neuroimaging, Institute of Neurology, University College London, London, UK) of MATLAB software (version R2013a for Windows, MathWorks, Natick, MA, USA). As described by Thomas et al.,[31] cortical GM/WM parcellation was performed using FreeSurfer software (version 6.0, Massachusetts General Hospital, Harvard Medical School; http://surfer.nmr.mgh.harvard.edu). This gyral parcellation is based on the Desikan–Killiany atlas for both the quantification and partial volume effect (PVE) correction of PET images. Region-based voxelwise PVE correction was performed using the symmetric geometric transfer matrix approach in the FreeSurfer software.[32] Voxel-based PVE correction was carried out using the ratio of the region-based PVE-corrected PET to its 7-mm-smoothed image.[28] Subcortical WM regions were segmented using cortical labels overlaid on the WM surface with voxels that were within a depth of 5 mm from the GM boundary. The mean standardized uptake value ratio (SUVR) was calculated for each volume of interest (VOI), based on the mean standardized uptake value (SUV) for each VOI, and was normalized to the mean SUV of cerebellar GM. SUVR thresholds of 1.32 and 0.62 for amyloid positivity were applied to [^{18}F]florbetaben and [^{18}F]flutemetamol PET scans, respectively.[33,34]

Acquisition and analysis of MRI data

MRI was performed with a 3.0-T system (Achieva, Philips Medical Systems, Best, The Netherlands) using an eight-channel sensitivity-encoding head coil at Asan Medical Center and Samsung Medical Center, or with the Magnetom Verio device (Siemens) with a Siemens matrix coil at Gil Medical Center.

We acquired T1-weighted multiecho magnetization-prepared rapid-acquisition gradient-echo structural images to evaluate the cortical thickness and volume, and T2-weighted fluid-attenuated inversion recovery images to evaluate the white-matter hyperintensity volume (WMHV). Images were analyzed using FreeSurfer software (version 6.0), and MRI parcellation was performed as described above.

Statistical analysis

Continuous variables are expressed as mean±standard-deviation

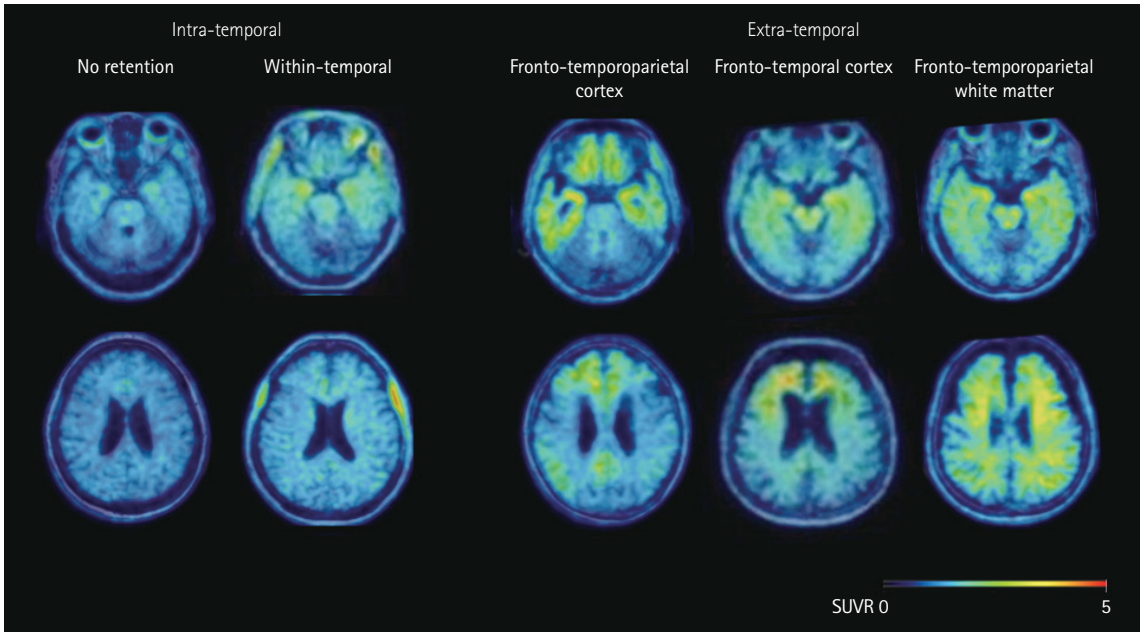

Fig. 1. Representative images of the standardized uptake value ratio (SUVR) for [^{18}F]THK-5351 in positron-emission tomography in amyloid-negative Alzheimer's disease. Retention patterns were visually classified into intratemporal spread (no retention or retention only within the temporal cortex [WT]) and extratemporal spread (retention in the frontotemporoparietal cortex [FTP], retention in the frontotemporal cortex, or diffuse retention in the frontotemporoparietal white matter rather than in the gray matter [FTP-WM]).

values or median and interquartile-range values, and categorical variables are expressed as frequencies. We applied chi-square or Fisher's exact tests to categorical variables and Kruskal–Wallis tests to quantitative variables. Statistical significance was defined as a two-sided p value<0.05. A Spearman's correlation analysis was performed to assess the correlation between variables. Statistical analyses were performed using Statistical Package for the Social Sciences (SPSS) software (version 18.0, SPSS Inc., Chicago, IL, USA).

RESULTS

Comparison between amyloid-positive and -negative AD

Among 164 patients with clinically probable AD, 23 (14.0%) were visually and quantitatively negative in [18F]florbetaben or [18F]flutemetamol PET. Patients with amyloid-negative AD were older (74.9±8.3 years vs. 67.2±10.6 years, p=0.001) and had a lower prevalence of early onset (onset age <65 years) (17.4% vs. 58.3%, p=0.001) compared with amyloid-positive AD. The prevalence of diabetes mellitus (DM) (39.1% vs. 10.6%, p<0.001) was significantly higher while the frequency of ApoE ε4 positivity was significantly lower (13.0% vs. 50.8%, p=0.001) in patients with amyloid-negative AD than in amyloid-positive AD.

Patients with amyloid-negative AD had an education duration of 7.5±5.4 years, a disease duration of 3.6±2.3 years, an MMSE score at baseline of 19.3±5.8, and a Clinical Dementia Rating (CDR) of 1.0±0.6. These patients had better visuospatial function and verbal and visual memory, and exhibited less color confusion than did patients with amyloid-positive AD. Demographics and the results of neuropsychological tests of the patients are summarized in Table 1. Complete neuropsychological data were available for only 120 of the 141 patients with amyloid-positive AD.

The mean cortical thickness and WMHV did not differ significantly between amyloid-positive and -negative AD. The hippocampal volume was smaller in patients with amyloid-positive AD (2,997.87±477.42 mm^3 vs. 3,334.78±637.60 mm^3, p=0.024). The global SUVR in amyloid PET was lower in patients with amyloid-negative AD than in amyloid-positive AD for both [18F]florbetaben (1.15±0.06 vs. 1.6±0.2, p<0.001) and [18F]flutemetamol (0.40±0.09 vs. 1.01±0.20, p<0.001).

Retention pattern of [18F]THK-5351 in amyloid-negative AD

Retention patterns of [18F]THK-5351 in amyloid-negative AD were classified as intratemporal spread in 10 patients (no retention: n=7, 30.4%; WT: n=3, 13.0%) and extratemporal spread in 13 patients (FTP: n=8, 34.8%; FT: n=3, 13.0%; FTP-WM: n=2, 8.7%) (Fig. 2).

The clinical and imaging characteristics according to the retention patterns of [18F]THK-5351 are summarized in Tables 1 and 2. Briefly, there was no statistically significant difference between the intra- and extratemporal spread groups in age (77.1±4.7 years vs. 73.2±10.2 years, p=0.927), education duration (7.9±5.8 years vs. 7.2±5.3 years, p=0.738, disease duration (3.9±2.9 years vs. 3.3±1.7 years, p=0.832), frequency of ApoE ε4 positivity (10.0% vs. 15.4%, p=0.602), MMSE score (20.4±4.3 vs. 18.4±6.8, p=0.738), CDR (0.8±0.3 vs. 1.1±0.8, p=0.784), CDR–Sum of Boxes (4.7±1.2 vs. 6.4±5.3, p=0.722), or Geriatric Depression Scale score (13.6±9.3 vs. 12.1±6.7, p=0.798). Patients with an extratemporal spread pattern in [18F]THK-5351 PET performed worse in verbal memory recognition tests than did patients with intratemporal retention (-2.19±1.50 vs. -0.77±1.07, p=0.048).

The cortical thickness (2.35±0.11 mm vs. 2.26±0.17 mm, p=0.251), hippocampal volume (3,273.43±595.03 vs. 3,381.98±688.63 mm^3, p=0.695), and WMHV (p=0.473) also did not differ significantly between the two groups. The global [18F]THK-5351 SUVR ($SUVR_{THK}$: 2.01±0.26 vs. 1.61±0.15, p=0.001) and $SUVR_{THK}$ in Braak stage III/IV (2.06±0.28 vs. 2.61±0.48, p=0.004) and Braak stage V/VI (1.60±0.14 vs. 2.00±0.23, p=0.001) were higher for extratemporal spread than for intratemporal spread.

Prognosis according to retention pattern of [18F]THK-5351 in amyloid-negative AD

Compared with the baseline value, the MMSE score at the 1-year follow-up had decreased in the extratemporal spread group but not in the intratemporal spread group (-3.5±3.2 vs. -0.5±2.8, p=0.020) (Table 3). After the PET scan, the clinical diagnosis remained unchanged in 56.5% (13 of 23) of the patients with amyloid-negative AD (Fig. 2). The rate of change in the diagnosis status did not differ significantly with the retention pattern (50.0% for intratemporal spread vs. 61.5% for extratemporal spread, p=0.580). The clinical diagnosis changed to FTD in 17.4% (n=4) of the patients with amyloid-negative AD: two of these patients had initially shown FTP retention patterns in PET and the other two had shown FT retention patterns. Therefore, the diagnosis changed to FTD in about one-third of the patients with the extratemporal spread pattern, whereas this did not occur in any of the patients with the intratemporal retention pattern. The remaining patients with changes in status (26.1%, n=6) were presumed to have subcortical vascular dementia (n=2), diffuse Lewy body dementia (n=2), or unclear etiology (n=2). The duration of follow-up was 25.0±14.1 months. The diagnosis had not altered at the follow-up in any of the patients.

DISCUSSION

Approximately 14% of the patients with clinical AD in this study were amyloid-negative, and most of these patients were also negative for ApoE ε4. About 70% of the patients with amyloid-negative AD in this study showed abnormal retention

Table 1. Demographics and the results of neuropsychological tests

	Comparison between amyloid (+) and amyloid (–) AD groups			Comparison within amyloid (–) AD group by retention pattern of THK-5351		
	Amyloid (+) AD (*n*=120)	Amyloid (–) AD (*n*=23)	*p*	Intra-temporal spread (*n*=10)	Extra-temporal spread (*n*=13)	*p*
Demographics						
Age (yr)	67.2±10.6	74.9±8.3	0.001	77.1±4.7	73.2±10.2	0.927
Sex, female	70.7	60.9	0.347	70.0	53.8	0.363
Education duration (yr)	8.9±4.7	7.5±5.4	0.240	7.9±5.8	7.2±5.3	0.738
Disease duration (yr)	4.1±2.4	3.6±2.3	0.349	3.9±2.9	3.3±1.7	0.832
Onset age <65 (yr)	58.3	17.4	0.001	0.0	30.8	0.054
Hypertension	28.5	43.5	0.152	40.0	46.2	0.552
Diabetes mellitus	10.6	39.1	<0.001	40.0	38.5	0.637
Hyperlipidemia	23.6	34.8	0.257	40.0	30.8	0.490
Hypothyroidism	0.0	8.7	0.125	0.0	15.4	0.308
Depression	7.7	4.3	0.626	10.0	0.0	0.435
Dementia family history	22.0	34.8	0.186	50.0	23.1	0.221
ApoE ε4 positivity	50.8	13.0	0.001	10.0	15.4	0.602
Neuropsychological tests						
MMSE score	18.0±5.6	19.3±5.8	0.347	20.4±4.3	18.4±6.8	0.738
CDR	0.9±0.6	1.0±0.6	0.727	0.8±0.3	1.1±0.8	0.784
CDR-Sum of Boxes	5.6±3.6	5.6±4.0	0.980	4.7±1.2	6.4±5.3	0.722
GDS score	12.3±7.9	12.9±7.9	0.412	13.6±9.3	12.1±6.7	0.798
Attention						
Digit Span Test, forward	-0.28±1.31	-0.08±0.97	0.406	-0.18±0.91	0.01±1.05	0.692
Digit Span Test, backward	-1.17±1.52	-0.41±2.09	0.122	-0.59±1.25	-0.24±2.69	0.888
Language and related function						
K-BNT	-2.20±2.32	-2.16±1.96	0.938	-1.60±1.42	-2.62±2.28	0.448
Visuospatial function						
RCFT, copying	-4.68±6.25	-1.38±2.29	0.016	-0.86±1.30	-1.81±2.86	0.644
Memory						
SVLT, immediate recall	-2.04±1.24	-1.48±0.90	0.046	-1.25±0.57	-1.67±1.09	0.322
SVLT, delayed recall	-2.35±0.80	-2.02±0.56	0.028	-1.99±0.43	-2.05±0.68	0.843
SVLT, recognition	-2.40±1.76	-1.54±1.49	0.023	-0.77±1.07	-2.19±1.50	0.048
RCFT, immediate recall	-1.80±0.86	-1.22±0.81	0.005	-1.20±0.71	-1.24±0.92	0.843
RCFT, delayed recall	-2.06±0.90	-1.39±0.71	<0.001	-1.30±0.64	-1.46±0.77	0.509
RCFT, recognition	-2.29±1.59	-1.23±1.24	0.001	-1.17±1.42	-1.28±1.14	0.895
Frontal executive function						
COWAT, animal names	-1.87±1.04	-1.84±0.82	0.868	-1.69±0.72	-1.96±0.92	0.510
COWAT, supermarket items	-1.56±0.98	-1.74±0.87	0.377	-1.65±0.85	-1.82±0.92	0.570
COWAT, phonemic fluency	-1.23±1.21	-0.98±0.82	0.258	-1.21±0.61	-0.77±0.95	0.288
Stroop test, color reading	-1.86±1.39	-1.12±1.10	0.042	-0.92±0.79	-1.35±1.42	0.668
TMT-B	-6.14±5.69	-4.06±5.00	0.202	-2.40±2.29	-5.26±6.19	0.807

Data are mean±standard-deviation values for continuous variables and percentage values for categorical variables. All data for neuropsychological tests are z scores.

AD, Alzheimer's disease; ApoE, apolipoprotein E; CDR, Clinical Dementia Rating; COWAT, Controlled Oral Word Association Test; GDS, Geriatric Depression Scale; K-BNT, Korean version of the Boston Naming Test; MMSE, Mini Mental State Examination; RCFT, Rey Complex Figure Test; SVLT, Seoul Verbal Learning Test; TMT-B, Trail-Making Test type B.

of [18F]THK-5351 in PET. We classified the retention patterns of [18F]THK-5351 into intra- and extratemporal spread according to the distribution of [18F]THK-5351 uptake in brain

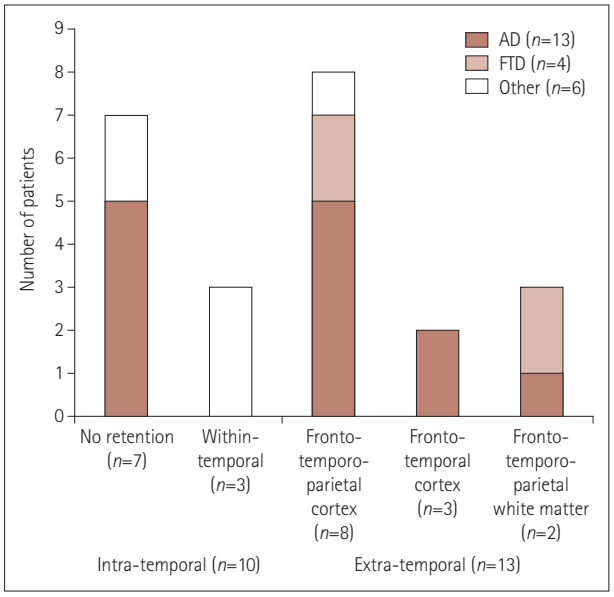

Fig. 2. Subgroups of postscan diagnoses according to visual patterns of [18F]THK-5351 retention in positron-emission tomography of patients with amyloid-negative Alzheimer's disease (AD). The clinical diagnosis remained unchanged as AD in five patients (50%) in the intratemporal group and changed to other diagnoses in the other members of that group (50%). The diagnosis remained unchanged as AD in eight patients (61.5%) in the extratemporal spread group, and changed to frontotemporal dementia (FTD) in four patients (30.8%) and other diagnoses in one patient (7.7%).

PET. The global and regional values of $SUVR_{THK}$ were higher in the extratemporal spread group than in the intratemporal group, and MMSE scores deteriorated rapidly during the follow-up only in the former. About half of the patients retained their clinical diagnosis of AD after [18F]THK-5351 PET.

Patients with amyloid-negative AD were older and had a lower frequency of ApoE-ε4-positive status than did patients with amyloid-positive AD (13.0% vs. 50.8%). Ward et al.[35] reported that the prevalence of ApoE ε4 positivity varied by geographic location, including from 38.48% to 45.27% among patients diagnosed with AD in Asia. This low proportion of ApoE ε4 positivity is consistent with the findings of a previous meta-analysis of the prevalence of amyloid PET positivity in dementia syndrome.[12] Although the ApoE ε4 allele has been recognized to be the strongest genetic risk factor for late-onset AD that acts via its effect on amyloid aggregation, clearance, and deposition onset,[36] late-onset AD is believed to be a complex, heterogeneous disease caused by multiple other genetic and environmental factors via diverse pathways.[37-39] Most of our patients with amyloid-negative AD showed abnormal retention of [18F]THK-5351 in PET. Although we could not confirm the specific etiology without performing an autopsy, this finding indicates that tau and neuroinflammation can contribute to the manifestation of clinical AD dementia, and is referred to as an AD phenocopy.

Patients with amyloid-negative AD were older and showed a higher prevalence of DM than did patients with amyloid-positive AD. The prevalence of DM increases with age,[40] and patients with late-onset AD often have concomitant cerebro-

Table 2. Imaging characteristics

	Comparison between amyloid (+) and amyloid (–) AD groups			Comparison within amyloid (–) AD group by retention pattern of THK-5351		
	Amyloid (+) AD (*n*=120)	Amyloid (–) AD (*n*=23)	*p*	Intra-temporal spread (*n*=10)	Extra-temporal spread (*n*=13)	*p*
MRI						
Cortical thickness (mm)	2.31±0.15	2.30±0.15	0.757	2.35±0.11	2.26±0.17	0.251
Hippocampal volume (mm^3)	2,997.87±477.42	3,334.78±637.60	0.024	3,273.43±595.03	3,381.98±688.63	0.695
Deep WMHV (mm^3)	493.37±879.10	675.65±941.66	0.380	718.00±979.57	643.08±950.45	0.855
PV WMHV (mm^3)	5,299.12±4,599.30	6,619.13±6,220.76	0.252	7,751.00±7,314.97	5,748.46±5,378.26	0.457
Total WMHV (mm^3)	5,792.50±5,207.38	7,293.04±6,702.01	0.243	8,469.00±7,989.41	6,388.46±5,695.25	0.473
Amyloid PET						
[18F]florbetaben SUVR, global	1.60±0.20	1.15±0.06	<0.001	1.17±0.01	1.13±0.07	0.251
[18F]flutemetamol SUVR, global	1.01±0.20	0.40±0.09	<0.001	0.37±0.03	0.44±0.13	0.522
THK-5351 PET						
SUVR, global		NA		1.61±0.15	2.01±0.26	0.001
SUVR, Braak stage I/II		NA		2.59±0.54	3.02±0.66	0.082
SUVR, Braak stage III/IV		NA		2.06±0.28	2.61±0.48	0.004
SUVR, Braak stage V/VI		NA		1.60±0.14	2.00±0.23	0.001

AD, Alzheimer's disease; MRI, magnetic resonance imaging; NA, not assessed; PET, positron-emission tomography; PV, periventricular; SUVR, standardized uptake value ratio; WMHV, white-matter hyperintensity volume.

Table 3. Prognosis according to retention pattern of [^{18}F]THK-5351 in patients with amyloid-negative PET

	Intratemporal spread (*n*=10)	Extratemporal spread (*n*=13)	*p*
MMSE score, baseline	20.4±4.3	18.4±6.8	0.738
MMSE score, 1-year follow-up	19.5±3.0	15.9±6.4	0.041
Δ(MMSE score), 1-year follow-up minus baseline	-0.5±2.8	-3.5±3.2	0.020

vascular disease pathologies as well as other neurodegenerative disease pathologies. These additional pathologies lower the threshold for the clinical diagnosis of AD,[41] and so the prevalence of amyloid positivity decreases with age.[12]

We classified patterns of [^{18}F]THK-5351 retention in PET into intra- and extratemporal spread patterns. When we compared the uptake of [^{18}F]THK-5351 in PET with that of the second-generation tau tracer [^{18}F]PI-2620, patients who showed an intratemporal uptake in [^{18}F]THK-5351 PET had negative findings for the latter.[42] This suggests that intratemporal [^{18}F]THK-5351 uptake was not due to the tau burden in the brain.

The group with an extratemporal spread of [^{18}F]THK-5351 retention was categorized into the FTP, FT, and FTP-WM patterns. Increased uptakes in the FTP in [^{18}F]THK-5351 PET were typically seen in patients with advanced AD, irrespective of their amyloid-negative status. This might be due to false-negative findings on amyloid PET scans reflecting the insensitivity of this technique in detecting advanced amyloid pathology, possibly caused by distinct conformations of amyloid plaques or marked atrophy.[43] However, this is probably only a partial explanation considering the high concordance between amyloid PET and pathology,[44] which further suggests that negative amyloid PET findings can rule out AD dementia. Furthermore, to remove the possibility of enrolling patients with near-threshold amyloid deposition, this study only enrolled patients with both visual and quantitative negative findings in amyloid PET. A possible explanation is that older people develop AD dementia in the presence of a low amyloid-β burden, which might not be detected by PET due to age-related diminished resilience (cognitive-reserve theory) or the cumulative effect of comorbid pathologies (double-hit hypothesis). Given the small numbers of participants in this study, further studies with large samples are needed to confirm this theory.

The second pattern of extratemporal spread involved increased uptake in the FT while sparing the parietal cortex, which was frequently seen in patients with FTD, including the behavioral variant of FTD (bvFTD) or the semantic variant of primary progressive aphasia (svPPA) in [^{18}F]THK-5351 PET.[32,45] Given that most svPPA cases are not tauopathies, the FT pattern of uptake is more likely to reflect neuroinflammation than true tau uptake. Furthermore, we found that patients with FTD who showed FT uptake of [^{18}F]THK-5351 showed no uptake of [^{18}F]PI-2620, which is a second-generation tau PET tracer.[42] Two-thirds of the patients in our study who showed this pattern had a diagnosis change from AD to FTD during the follow-up period, which suggests that [^{18}F]THK-5351 uptake pattern can reflect the clinical course.

The third pattern of extratemporal spread involved diffusely increased uptake, predominantly in the WM. We previously reported that the uptake of [^{18}F]THK-5351 in the GM and WM during PET differs between bvFTD and other types of dementia, including AD.[28] The increased uptake in the frontal WM was greater than that in the GM, and correlated with executive function, which suggests that [^{18}F]THK-5351 uptake in the WM reflects neuropathological differences between bvFTD and other types of dementia. However, long-term follow-up is needed to confirm this hypothesis, since the patients exhibiting this uptake pattern were still clinically considered to have AD dementia during the short follow-up period in the present study.

Dementia represents the clinically observable outcome of the cumulative burden of multiple pathological insults in the brain. Although the most common pathology is AD,[46] most older patients with dementia have multiple underlying pathological changes. Accurately determining the cause of dementia while patients are alive is essential for developing and implementing disease-specific therapies, but a diagnosis based on clinical criteria alone is generally insufficient for determining the histopathological cause of dementia.[4] Amyloid PET can be used to measure the amount of amyloid-β aggregates—one of the pathological hallmarks of AD[8-11]—in the brains of living subjects. Nevertheless, 16%–39% of subjects with suspected AD have been found to have amyloid-negative findings.[47-49] However, a negative visual interpretation cannot rule out the presence of amyloid and tau levels sufficiently to support a classification of moderate AD neuropathological changes.[27]

We explored the clinical and imaging characteristics of the patients with amyloid-negative AD using currently available tests. About half of the patients in this study retained an AD diagnosis, regardless of the type of retention pattern in [^{18}F]THK-5351 PET. One-sixth of patients in whom the diagnosis changed to FTD showed an extratemporal spread. The remaining patients were presumed to have other diseases, including subcortical vascular dementia and diffuse Lewy body dementia, based on amyloid- and tau-negative patterns as well as the clinical follow-up. Most of these patients exhibited an

intratemporal retention pattern in [18F]THK-5351 PET.

While we could not establish the specific etiology, we did find that patients with extensive [18F]THK-5351 retention beyond the temporal lobe exhibited rapid deterioration in their MMSE scores, which suggests that neuroinflammation can accelerate the clinical progression of various types of neurodegenerative disease. This is consistent with the previous finding that [18F]THK-5351 can predict cognitive decline or the conversion to AD in patients with mild cognitive impairment.[50,51]

There were several limitations in this study. First, there were relatively few patients with amyloid-negative AD. This could have been responsible for the lack of significant differences in clinical characteristics and cognitive function scores between the intra- and extratemporal spread groups. Further studies with larger populations are therefore needed to confirm the characteristics of amyloid-negative AD. Second, the follow-up period might have been too short to make a definite diagnosis. Moreover, the diagnosis was not confirmed pathologically by autopsy. However, the diagnosis was established by utilizing all currently available clinical and imaging tests, other than pathological confirmation, which is impossible in living patients. Finally, none of the study subjects underwent follow-up detailed neuropsychological tests, and so we could not evaluate the disease progression precisely.

In conclusion, we have identified the clinical characteristics and [18F]THK-5351 uptake patterns in clinical AD dementia with negative findings for amyloid in PET. [18F]THK-5351 PET imaging assesses both astrogliosis and tau, and may be useful for discriminating neurodegenerative diseases regardless of the amyloid PET findings.

Availability of Data and Material

The datasets generated or analyzed during the study are available from the corresponding author on reasonable request.

ORCID iDs

Minyoung Oh	https://orcid.org/0000-0002-6840-3215
Jungsu S. Oh	https://orcid.org/0000-0002-1925-8103
Seung Jun Oh	https://orcid.org/0000-0002-3769-067X
Sang Ju Lee	https://orcid.org/0000-0002-2137-4410
Jee Hoon Roh	https://orcid.org/0000-0002-3243-0529
Woo Ram Kim	https://orcid.org/0000-0003-1361-4426
Ha-Eun Seo	https://orcid.org/0000-0003-4452-0908
Jae Myeong Kang	https://orcid.org/0000-0003-0803-9332
Sang Won Seo	https://orcid.org/0000-0002-8747-0122
Jae-Hong Lee	https://orcid.org/0000-0001-7368-4560
Duk L. Na	https://orcid.org/0000-0002-0098-7592
Young Noh	https://orcid.org/0000-0002-9633-3314
Jae Seung Kim	https://orcid.org/0000-0003-1710-1185

Author Contributions

Conceptualization: Minyoung Oh, Young Noh, Jae Seung Kim. Data curation: all authors. Formal analysis: all authors. Funding acquisition: Young Noh, Jae Seung Kim. Investigation: Woo Ram Kim, Ha-Eun Seo. Methodology: Jungsu S. Oh, Young Noh. Resources: Jee Hoon Roh, Jae-Hong Lee, Sang Ju Lee, Seung Jun Oh, Sang Won Seo, Jae Myeong Kang, Young Noh. Supervision: Jee Hoon Roh, Jae-Hong Lee, Sang Won Seo, Duk L. Na, Young Noh. Visualization: Woo Ram Kim, Ha-Eun Seo, Jungsu S. Oh. Writing—original draft: Minyoung Oh, Young Noh, Jae Seung Kim. Writing—review & editing: all authors.

Conflicts of Interest

The authors have no potential conflicts of interest to disclose.

Funding Statement

This research was supported by a grant from the Korea Health Technology R&D Project through the Korea Health Industry Development Institute, funded by the Ministry of Health & Welfare, Republic of Korea (grant number: HI14C2768, HI18C2383, and HI14C1135), by the Brain Research Program of the National Research Foundation funded by the Korean government (No. 2018M3C7A1056889), and by the National Research Foundation of Korea (NRF) grant funded by the Korea government (MSIT) (No. 2021R1A2C3009056).

REFERENCES

1. Alzheimer's Association. Alzheimer's disease facts and figures. *Alzheimers Dement* 2020;16:391-460.
2. Prince MJ, Wimo A, Guerchet MM, Ali GC, Wu YT, Prina M. *World Alzheimer report 2015 the global impact of dementia: an analysis of prevalence, incidence, cost & trends*. London: Alzheimer's Disease International, 2015.
3. McKhann GM, Knopman DS, Chertkow H, Hyman BT, Jack CR Jr, Kawas CH, et al. The diagnosis of dementia due to Alzheimer's disease: recommendations from the National Institute on Aging-Alzheimer's Association workgroups on diagnostic guidelines for Alzheimer's disease. *Alzheimers Dement* 2011;7:263-269.
4. Beach TG, Monsell SE, Phillips LE, Kukull W. Accuracy of the clinical diagnosis of Alzheimer disease at National Institute on Aging Alzheimer Disease Centers, 2005-2010. *J Neuropathol Exp Neurol* 2012;71:266-273.
5. Knopman DS, DeKosky ST, Cummings JL, Chui H, Corey-Bloom J, Relkin N, et al. Practice parameter: diagnosis of dementia (an evidence-based review). Report of the Quality Standards Subcommittee of the American Academy of Neurology. *Neurology* 2001;56:1143-1153.
6. Salloway S, Sperling R, Fox NC, Blennow K, Klunk W, Raskind M, et al. Two phase 3 trials of bapineuzumab in mild-to-moderate Alzheimer's disease. *N Engl J Med* 2014;370:322-333.
7. Doody RS, Thomas RG, Farlow M, Iwatsubo T, Vellas B, Joffe S, et al. Phase 3 trials of solanezumab for mild-to-moderate Alzheimer's disease. *N Engl J Med* 2014;370:311-321.
8. Klunk WE, Engler H, Nordberg A, Wang Y, Blomqvist G, Holt DP, et al. Imaging brain amyloid in Alzheimer's disease with Pittsburgh Compound-B. *Ann Neurol* 2004;55:306-319.
9. Barthel H, Gertz HJ, Dresel S, Peters O, Bartenstein P, Buerger K, et al. Cerebral amyloid-β PET with florbetaben (18F) in patients with Alzheimer's disease and healthy controls: a multicentre phase 2 diagnostic study. *Lancet Neurol* 2011;10:424-435.
10. Vandenberghe R, Van Laere K, Ivanoiu A, Salmon E, Bastin C, Triau E, et al. 18F-flutemetamol amyloid imaging in Alzheimer disease and mild cognitive impairment: a phase 2 trial. *Ann Neurol* 2010;68:319-329.
11. Clark CM, Schneider JA, Bedell BJ, Beach TG, Bilker WB, Mintun MA, et al. Use of florbetapir-PET for imaging beta-amyloid pathology. *JAMA* 2011;305:275-283.
12. Ossenkoppele R, Jansen WJ, Rabinovici GD, Knol DL, van der Flier WM, van Berckel BN, et al. Prevalence of amyloid PET positivity in dementia syndromes: a meta-analysis. *JAMA* 2015;313:1939-1949.

13. Barkhof F, Polvikoski TM, van Straaten EC, Kalaria RN, Sulkava R, Aronen HJ, et al. The significance of medial temporal lobe atrophy: a postmortem MRI study in the very old. *Neurology* 2007;69:1521-1527.
14. Serrano-Pozo A, Qian J, Monsell SE, Blacker D, Gómez-Isla T, Betensky RA, et al. Mild to moderate Alzheimer dementia with insufficient neuropathological changes. *Ann Neurol* 2014;75:597-601.
15. Crary JF, Trojanowski JQ, Schneider JA, Abisambra JF, Abner EL, Alafuzoff I, et al. Primary age-related tauopathy (PART): a common pathology associated with human aging. *Acta Neuropathol* 2014;128:755-766.
16. Harada R, Okamura N, Furumoto S, Furukawa K, Ishiki A, Tomita N, et al. 18F-THK5351: a novel PET radiotracer for imaging neurofibrillary pathology in Alzheimer disease. *J Nucl Med* 2016;57:208-214.
17. Harada R, Ishiki A, Kai H, Sato N, Furukawa K, Furumoto S, et al. Correlations of 18F-THK5351 PET with postmortem burden of tau and astrogliosis in Alzheimer disease. *J Nucl Med* 2018;59:671-674.
18. Ng KP, Pascoal TA, Mathotaarachchi S, Therriault J, Kang MS, Shin M, et al. Monoamine oxidase B inhibitor, selegiline, reduces 18F-THK5351 uptake in the human brain. *Alzheimers Res Ther* 2017;9:25.
19. McKhann G, Drachman D, Folstein M, Katzman R, Price D, Stadlan EM. Clinical diagnosis of Alzheimer's disease: report of the NINCDS-ADRDA Work Group under the auspices of Department of Health and Human Services Task Force on Alzheimer's disease. *Neurology* 1984;34:939-944.
20. Noh Y, Lee Y, Seo SW, Jeong JH, Choi SH, Back JH, et al. A new classification system for ischemia using a combination of deep and periventricular white matter hyperintensities. *J Stroke Cerebrovasc Dis* 2014;23:636-642.
21. Kang Y, Na DL, Hahn S. *Seoul Neuropsychological Screening Battery.* Incheon: Human Brain Research & Consulting Co., 2003.
22. Rascovsky K, Hodges JR, Knopman D, Mendez MF, Kramer JH, Neuhaus J, et al. Sensitivity of revised diagnostic criteria for the behavioural variant of frontotemporal dementia. *Brain* 2011;134:2456-2477.
23. Román GC, Erkinjuntti T, Wallin A, Pantoni L, Chui HC. Subcortical ischaemic vascular dementia. *Lancet Neurol* 2002;1:426-436.
24. McKeith IG, Galasko D, Kosaka K, Perry EK, Dickson DW, Hansen LA, et al. Consensus guidelines for the clinical and pathologic diagnosis of dementia with Lewy bodies (DLB): report of the consortium on DLB international workshop. *Neurology* 1996;47:1113-1124.
25. McKeith IG, Dickson DW, Lowe J, Emre M, O'Brien JT, Feldman H, et al. Diagnosis and management of dementia with Lewy bodies: third report of the DLB consortium. *Neurology* 2005;65:1863-1872.
26. Joshi A, Koeppe RA, Fessler JA. Reducing between scanner differences in multi-center PET studies. *Neuroimage* 2009;46:154-159.
27. Sonni I, Lesman Segev OH, Baker SL, Iaccarino L, Korman D, Rabinovici GD, et al. Evaluation of a visual interpretation method for tau-PET with 18F-flortaucipir. *Alzheimers Dement (Amst)* 2020;12:e12133.
28. Son HJ, Oh JS, Roh JH, Seo SW, Oh M, Lee SJ, et al. Differences in gray and white matter 18F-THK5351 uptake between behavioral-variant frontotemporal dementia and other dementias. *Eur J Nucl Med Mol Imaging* 2019;46:357-366.
29. Piramal Imaging. NEURACEQ (florbetaben F 18 injection), for intravenous use: prescribing information [Internet]. Matran: Piramal Imaging; 2014 [cited 2021 Jun 8]; Available from: https://www.accessdata.fda.gov/drugsatfda_docs/label/2014/204677s000lbl.pdf.
30. GE Healthcare. Vizamyl (flutemetamol F 18 injection) for intravenous use: prescribing information [Internet]. Arlington Heights: GE Healthcare; 2013 Revised Feb. 2017 [cited 2021 Jun 8]; Available from: https://www.accessdata.fda.gov/drugsatfda_docs/label/2017/203137s008lbl.pdf.
31. Thomas BA, Erlandsson K, Modat M, Thurfjell L, Vandenberghe R, Ourselin S, et al. The importance of appropriate partial volume correction for PET quantification in Alzheimer's disease. *Eur J Nucl Med Mol Imaging* 2011;38:1104-1119.
32. Sattarivand M, Kusano M, Poon I, Caldwell C. Symmetric geometric transfer matrix partial volume correction for PET imaging: principle, validation and robustness. *Phys Med Biol* 2012;57:7101-7116.
33. Son HJ, Oh JS, Oh M, Kim SJ, Lee JH, Roh JH, et al. The clinical feasibility of deep learning-based classification of amyloid PET images in visually equivocal cases. *Eur J Nucl Med Mol Imaging* 2020;47:332-341.
34. Thurfjell L, Lilja J, Lundqvist R, Buckley C, Smith A, Vandenberghe R, et al. Automated quantification of 18F-flutemetamol PET activity for categorizing scans as negative or positive for brain amyloid: concordance with visual image reads. *J Nucl Med* 2014;55:1623-1628.
35. Ward A, Crean S, Mercaldi CJ, Collins JM, Boyd D, Cook MN, et al. Prevalence of apolipoprotein E4 genotype and homozygotes (APOE e4/4) among patients diagnosed with Alzheimer's disease: a systematic review and meta-analysis. *Neuroepidemiology* 2012;38:1-17.
36. Altamura C, Squitti R, Pasqualetti P, Tibuzzi F, Silvestrini M, Ventriglia MC, et al. What is the relationship among atherosclerosis markers, apolipoprotein E polymorphism and dementia? *Eur J Neurol* 2007;14:679-682.
37. Efthymiou AG, Goate AM. Late onset Alzheimer's disease genetics implicates microglial pathways in disease risk. *Mol Neurodegener* 2017;12:43.
38. Profenno LA, Porsteinsson AP, Faraone SV. Meta-analysis of Alzheimer's disease risk with obesity, diabetes, and related disorders. *Biol Psychiatry* 2010;67:505-512.
39. Karch CM, Goate AM. Alzheimer's disease risk genes and mechanisms of disease pathogenesis. *Biol Psychiatry* 2015;77:43-51.
40. Menke A, Casagrande S, Geiss L, Cowie CC. Prevalence of and trends in diabetes among adults in the United States, 1988-2012. *JAMA* 2015;314:1021-1029.
41. Kapasi A, DeCarli C, Schneider JA. Impact of multiple pathologies on the threshold for clinically overt dementia. *Acta Neuropathol* 2017;134:171-186.
42. Oh M, Oh SJ, Lee SJ, Oh JS, Roh JH, Chung SJ, et al. Clinical evaluation of 18F-PI-2620 as a potent PET radiotracer imaging tau protein in Alzheimer disease and other neurodegenerative diseases compared with 18F-THK-5351. *Clin Nucl Med* 2020;45:841-847.
43. Bullich S, Seibyl J, Catafau AM, Jovalekic A, Koglin N, Barthel H, et al. Optimized classification of 18F-Florbetaben PET scans as positive and negative using an SUVR quantitative approach and comparison to visual assessment. *Neuroimage Clin* 2017;15:325-332.
44. Sabri O, Sabbagh MN, Seibyl J, Barthel H, Akatsu H, Ouchi Y, et al. Florbetaben PET imaging to detect amyloid beta plaques in Alzheimer's disease: phase 3 study. *Alzheimers Dement* 2015;11:964-974.
45. Jang YK, Lyoo CH, Park S, Oh SJ, Cho H, Oh M, et al. Head to head comparison of [18F] AV-1451 and [18F] THK5351 for tau imaging in Alzheimer's disease and frontotemporal dementia. *Eur J Nucl Med Mol Imaging* 2018;45:432-442.
46. White L, Small BJ, Petrovitch H, Ross GW, Masaki K, Abbott RD, et al. Recent clinical-pathologic research on the causes of dementia in late life: update from the Honolulu-Asia Aging Study. *J Geriatr Psychiatry Neurol* 2005;18:224-227.
47. Apostolova LG, Haider JM, Goukasian N, Rabinovici GD, Chételat G, Ringman JM, et al. Critical review of the appropriate use criteria for amyloid imaging: effect on diagnosis and patient care. *Alzheimers Dement (Amst)* 2016;5:15-22.
48. Boccardi M, Altomare D, Ferrari C, Festari C, Guerra UP, Paghera B, et al. Assessment of the incremental diagnostic value of florbetapir F 18 imaging in patients with cognitive impairment: the incremental diagnostic value of amyloid PET with [18F]-florbetapir (INDIA-FBP) study. *JAMA Neurol* 2016;73:1417-1424.
49. Rabinovici GD, Gatsonis C, Apgar C, Chaudhary K, Gareen I, Hanna L, et al. Association of amyloid positron emission tomography with subsequent change in clinical management among medicare

beneficiaries with mild cognitive impairment or dementia. *JAMA* 2019;321:1286-1294.
50. Jeong HJ, Lee H, Lee SY, Seo S, Park KH, Lee YB, et al. [18F] THK5351 PET imaging in patients with mild cognitive impairment. *J Clin Neurol* 2020;16:202-214.
51. Lee HJ, Lee EC, Seo S, Ko KP, Kang JM, Kim WR, et al. Identification of heterogeneous subtypes of mild cognitive impairment using cluster analyses based on PET imaging of tau and astrogliosis. *Front Aging Neurosci* 2021;12:615467.